Mycobacteria tolerate carbon monoxide by remodelling their respiratory chain

Katherine Bayly[a,b], Paul R. F. Cordero[a,b], Cheng Huang[c], Ralf B. Schittenhelm[c], Rhys Grinter[a,b]*, Chris Greening[a,b]*

[a] Department of Microbiology, Monash Biomedicine Discovery Institute, Monash University, Clayton, VIC 3800, Australia

[b] School of Biological Sciences, Monash University, Clayton, VIC 3800, Australia

[c] Monash Proteomics and Metabolomics Facility and Department of Biochemistry, Monash Biomedicine Discovery Institute, Monash University, Clayton, VIC 3800, Australia

* Correspondence can be addressed to:

Associate Professor Chris Greening (chris.greening@monash.edu)

Dr Rhys Grinter (rhys.grinter@monash.edu)

Abstract word count: 214

Total word count: 4904

Abstract

Carbon monoxide (CO) is a gas infamous for its acute toxicity. The toxicity of CO predominantly stems from its tendency to form carbonyl complexes with transition metals, thus inhibiting the heme-prosthetic groups of proteins, including the terminal oxidases of the respiratory chain. While CO has been proposed as an antibacterial agent, the evidence supporting its toxicity towards bacteria is equivocal, and its cellular targets remain poorly defined. In this work, we investigate the physiological response of mycobacteria to CO. We show that *Mycobacterium smegmatis* is highly resistant to the toxic effects of CO, exhibiting normal growth parameters when cultured in its presence. We profiled the proteome of *M. smegmatis* during growth in CO, identifying strong induction of cytochrome *bd* oxidase and members of the *dos* regulon, but relatively few other changes. We show that the activity of cytochrome *bd* oxidase is resistant to CO, whereas cytochrome *bcc-aa*$_3$ oxidase is strongly inhibited by this gas. Consistent with these findings, growth analysis shows that *M. smegmatis* lacking cytochrome *bd* oxidase displays a significant growth defect in the presence of CO, while induction of the *dos* regulon appears to be unimportant for adaption to CO. Altogether, our findings suggest that *M. smegmatis* has considerable resistance to CO and benefits from respiratory flexibility to withstand its inhibitory effects.

Importance

Carbon monoxide has an infamous reputation as a toxic gas and it has been suggested that it has potential as an antibacterial agent. Despite this, the means by which bacteria resist its toxic effects are not well understood. In this study we determine the physiological response of *Mycobacterium smegmatis* to growth in CO.

We show for the first time that the cytochrome *bd* oxidase is inherently resistant to CO and is deployed by *M. smegmatis* to tolerate the presence of this gas. Further, we show that aside from this remodelling of its respiratory chain, *M. smegmatis* makes few other functional changes to its proteome, suggesting it has a high level of inherent resistance to CO.

Introduction

Carbon monoxide (CO) is notorious as a noxious gas, largely due to the acute toxicity observed in humans and higher vertebrates upon inhalation (1). However, while CO is an energy-rich molecule that can be oxidized to yield low-potential electrons, it is largely chemically inert under physiological conditions (2). The toxicity of CO stems from its tendency to form carbonyl complexes with transition metals (3), specifically the Fe ion of heme groups, which are indispensable for many biochemical processes (4). Despite considerable knowledge of the chemistry of CO-metal interactions, the specific cellular targets of CO toxicity are still only partially defined (5). Toxicity at a cellular level is thought to arise primarily from competitive inhibition of heme-containing respiratory enzymes, i.e. heme-copper terminal oxidases; however, given the abundance of heme-containing proteins in most cells, this is unlikely to be the sole target (6).

While CO is acutely toxic to mammals, the evidence demonstrating this gas is also potently toxic towards bacteria is equivocal. A number of studies working with diverse bacterial species have demonstrated that, while gaseous CO is inhibitory to bacteria, this inhibition is only observed at high CO partial pressures (2-30%), is transient, and acts to slow rather than halt bacterial growth (7-10). Studies treating bacteria with CO-releasing molecules (CORMs) have reported more acute toxicity and a bactericidal mode of action, which was attributed to CO (10, 11). However, subsequent analysis of the effect of CORMs strongly suggests that this toxicity is largely due to the transition metal complex that constitutes many CORMs, rather than toxicity of CO (12, 13). Further investigation is required to determine the extent to which CO is toxic to bacteria, the molecular targets of toxicity, and how bacteria are able to grow at high partial pressures of CO.

The role of CO in the physiology of *Mycobacterium* has remained controversial. This diverse actinobacterial genus includes saprophytic species such as *Mycobacterium smegmatis*, which are prevalent in soils (14). The genus also includes numerous human and animal pathogens, including *Mycobacterium tuberculosis,* the causative agent of tuberculosis, which is currently the world's deadliest infectious disease (15). Mycobacterial species, including *M. smegmatis* and *M. tuberculosis,* seem to be relatively resistant to CO and exhibit robust growth in the presence of a 20-30% CO atmosphere (8, 16). Furthermore, both *M. smegmatis* and *M. tuberculosis* possess the enzyme CO dehydrogenase to use CO as an energy source; it was recently demonstrated that *M. smegmatis* enhances its long-term survival by scavenging atmospheric CO when exhausted for preferred organic energy sources (9).

Mycobacteria are obligate aerobes, meaning they require a functioning aerobic respiratory chain to grow (17). As a result, the inhibitory effect of CO on the oxygen-binding heme groups of the terminal oxidases must be resisted for these bacteria to grow in the presence of CO. The mycobacterial respiratory chain is branched, with the final reduction of molecular oxygen mediated by one of two terminal oxidases: the cytochrome *bcc-aa*$_3$ complex or cytochrome *bd* oxidase (18). The cytochrome *bcc-aa*$_3$ complex is a supercomplex composed of components analogous to mitochondrial complex III and IV; it is primarily synthesized under optimal growth conditions (19) and is the more efficient of the two oxidases given it acts as a proton pump (18). Alternatively, cytochrome *bd* oxidase is non-proton pumping and is therefore less efficient, but is thought to have a higher O_2 affinity and is induced during hypoxia (20, 21). Cytochrome *aa*$_3$ oxidases are members of the heme-copper oxidase superfamily with binuclear heme-copper active sites that are highly susceptible to inhibition by ligands like CO, nitric oxide (NO), cyanide (CN^-) and

hydrogen sulphide (H_2S) (22). Cytochrome *bd* oxidases are unrelated to heme-copper oxidases and utilise dual *b* and *d* hemes in their active site for O_2 reduction (21). In a number of bacteria, cytochrome *bd* oxidase is important for resistance to oxidative and nitrosative stress, as well as to NO, CN and H_2S, suggesting its active site is less susceptible to inhibition by non-O_2 ligands (23-25). However, it remains to be determined whether it plays a similar role in bacterial resistance to CO.

In addition to acting as an alternative energy source at low concentrations and respiratory toxin at high concentrations, CO has been shown to influence gene expression in mycobacteria, via the two-component DosS/DosR system (8, 26). The sensor histidine kinase DosS is a hemoprotein that activates the transcriptional regulator DosR via phosphorylation in response to low oxygen, low redox state or via binding of ligands to its heme functional group (27). The DosS/DosR regulator has been most thoroughly characterized in *M. tuberculosis*, which possesses an additional sensor kinase designated DosT that acts synergistically with DosS to modulate DosR function (28). In *M. tuberculosis*, the *dos* regulon contains 48 genes and contributes to survival during hypoxia-induced dormancy (27, 29, 30). While the Dos response plays a role in adaption to hypoxia and for resistance to respiratory inhibition by NO, the physiological role of its activation in response to CO in *M. tuberculosis* has not been determined (8, 26, 30). Moreover, in *M. tuberculosis*, *dos* activation in response to CO is much less pronounced than to NO and may potentially be a non-specific effect relating to the inherent affinity of CO for heme functional groups (8). In *M. smegmatis*, the *dos* regulon plays a similar role to *M. tuberculosis* in preparing cells for hypoxia and is largely analogous, with the notable addition of the hydrogenases Hhy and Hyh, which are responsible respectively for the oxidation hydrogen as an energy source and for fermentative hydrogen

123 production (17, 31-33). The activation of the *dos* response by CO and a potential role
124 in CO resistance in *M. smegmatis* has not previously been investigated.

125 In this study, we sought to determine the effect of CO on *M. smegmatis* throughout
126 its growth cycle. To achieve this goal, we combined systematic analysis of *M.*
127 *smegmatis* growth in the presence of CO with whole-cell shotgun proteomics to
128 determine the response of *M. smegmatis* to growth in CO at the protein level. To
129 place these data in a functional context, we utilised terminal oxidase mutants to
130 directly determine the ability of the *M. smegmatis* terminal oxidases to support
131 respiration and growth in the presence of CO. Our results show that *M. smegmatis*
132 utilises cytochrome *bd* oxidase as a primary means of resisting inhibition of its
133 respiratory chain by CO. The mutant strain lacking cytochrome *bd* oxidase is
134 impaired in its ability to grow in the presence of CO. Cytochrome *bd* oxidase is
135 induced during growth in CO, and its oxidase activity is resistant to the presence of
136 CO. These data provide the first direct evidence of the role of this terminal oxidase in
137 resistance to CO in mycobacteria.

138

139 # Results

140 ## *M. smegmatis* induces cytochrome *bd* oxidase and the *dos* regulon during
141 ## growth in the presence of CO

142 In order to determine the effect of CO on *M. smegmatis*, we systematically compared
143 the growth of wild-type *M. smegmatis* in glycerol-containing minimal media in sealed
144 vials, under an atmosphere with either 20% N_2 or 20% CO. Growth of *M. smegmatis*
145 was slightly slower in the presence of 20% CO (Figure 1A), though exponential-

146 phase growth rate and final growth yield were near-identical under both conditions
147 (Figure 1B, D). The lag phase during growth in 20% CO was 1.3-fold longer than in
148 20% N_2, accounting for the slight difference in growth. This suggests that *M.*
149 *smegmatis* is initially inhibited by CO, but grows normally after adapting to the gas,
150 likely through gene expression changes (Figure 1C). In order to identify changes in
151 the *M. smegmatis* proteome that may account for this adaption to CO, we performed
152 proteomic analysis on *M. smegmatis* cultures in the presence and absence of 20%
153 CO during mid-exponential phase.

154 Proteomic analysis showed that 37 proteins are differentially abundant in response
155 to growth in the presence of 20% CO, with 27 proteins more abundant and 10 less
156 abundant (Figure 2A, Table S1). The cytochrome *bd* oxidase subunits CydA and
157 CydB were highly induced (24- and 4.8-fold) in response to growth in 20% CO, while
158 levels of cytochrome *bcc-aa*$_3$ (QcrCAB) were unaffected (Figure 2A, Table S1). This
159 suggests that in mycobacteria, cytochrome *bd* oxidase is induced to adapt to growth
160 in CO and may be inherently resistant to inhibition by this gas. This is consistent with
161 previous observations that other bacteria deploy cytochrome *bd* oxidase to cope with
162 inhibition of cytochrome *aa*$_3$-type heme-copper oxidases by gaseous molecules like
163 NO, CN and H_2S (23-25). Fifteen of the most induced proteins belong to the *dos*
164 regulon, representing a subset the regulon, which includes the regulator of the
165 pathway DosR (5.0-fold), universal stress protein family proteins (98 to 5.7-fold), and
166 Acg (1007-fold) and Fsq (72-fold), two proteins that protect against oxidative stress
167 through the sequestration of flavins (34, 35). The full *dos* regulon in *M. smegmatis*
168 contains 49 proteins (17). Notable *dos*-regulated proteins not induced by CO include
169 the hydrogenases Hhy or Hyh, which are important for the response to starvation
170 and hypoxia respectively (17, 36).

171 There were fewer proteins with decreased abundance in response to CO exposure.
172 The ESX-3 type-VII secretion system component EccC3, known to be involved in the
173 export of proteins important for iron acquisition (37), exhibited the largest decrease in
174 abundance (15-fold). Correlating with this, the acyl-dehydrogenase MbtN involved in
175 synthesis of the iron binding siderophore mycobactin (38) was also less abundant
176 (10-fold). The decreased abundance of proteins involved in iron acquisition suggests
177 that *M. smegmatis* does not experience iron-limitation during growth in CO, due to
178 iron sequestration in Fe-carbonyl complexes. Iron limitation induced by this
179 mechanism was proposed for *E. coli*, which was shown to transcriptionally
180 upregulate iron-acquisition systems in response to CO (39).

181 The 37 proteins with differential abundance in response to CO comprise only 0.56%
182 of the total 6,625 proteins predicted to be synthesized by *M. smegmatis* mc^2155 (40).
183 This is in contrast to *E. coli*, where 20% of genes were shown to be differentially
184 regulated at a transcriptional level 80 minutes after exposure CO gas (39). This
185 suggests that *M. smegmatis* has a high level of inherent resistance to CO toxicity,
186 requiring relatively few changes to its proteome to cope with this gas. Among
187 proteins that were not differentially abundant during growth in CO were Cor and CO
188 dehydrogenase. Cor was reported to be the most important gene for CO resistance
189 in *M. tuberculosis* (41), and is highly conserved in *M. smegmatis* (MSMEG_3645,
190 94% amino acid identity); while the exact function of this protein remains unresolved,
191 this results suggests Cor-mediated CO resistance is independent of induction by CO.
192 The lack of induction of CO dehydrogenase in response to CO is consistent with
193 previous findings that this enzyme is deployed to utilise trace quantities of CO as an
194 energy source during persistence (9).

195

196 **Cytochrome *bd* oxidase, but not DosR, contributes to CO resistance**

197 Our proteomic analysis demonstrates that *M. smegmatis* induces cytochrome *bd*
198 oxidase and members of the *dos* regulon in response to CO. To determine the role
199 of the terminal oxidases and the *dos* regulon in resistance to CO, we systematically
200 assessed the growth of *M. smegmatis* strains with genetic deletions to the
201 cytochrome *bcc-aa*$_3$ oxidase (Δ*qcrCAB*), cytochrome *bd* oxidase *(ΔcydAB)*, and the
202 regulator DosR (*ΔdosR)*, as above, in the presence of 20% CO or 20% N_2. Growth of
203 the *ΔdosR* strain was identical to wild-type in both the N_2- and CO-supplemented
204 conditions (Figure 1A). This shows that the inability of the *ΔdosR* strain to induce
205 the *dos* regulon has no effect on growth in CO and suggests that the partial induction
206 of the *dos* regulon by CO is a non-specific rather than adaptive response.

207 There were significant differences in the growth characteristics of the terminal
208 oxidase mutants in the presence and absence of CO. In line with previous
209 observations (42), the Δ*qcrCAB* mutant exhibited a longer lag phase, slower specific
210 growth rate, and lower final growth yield compared to the wild-type, whereas the
211 *ΔcydAB* mutant exhibited only minor growth defects (Figure 1A-C). The growth of the
212 Δ*qcrCAB* strain did not differ in the presence and absence of CO, suggesting that
213 cytochrome *bd* oxidase is inherently resistant to inhibition by CO (Figure 1A-D). In
214 contrast, the *ΔcydAB* strain grew markedly slower in the presence of CO compared
215 to growth in the 20% N_2-amended control. This slower growth is largely attributable
216 to an increase in lag phase, as the specific growth rate of the *ΔcydAB* strain during
217 exponential phase in CO was only slightly lower than wild-type (Figure 1B). The
218 increase in lag phase of the *ΔcydAB* strain in CO was 2.5-fold longer than for wild-

type *M. smegmatis* (Figure 1C). This is consistent with our proteomic analysis that shows cytochrome *bd* oxidase is induced in response to CO, and demonstrates that this terminal oxidase is important for adaptation to growth in CO. Interestingly, final growth yield was significantly higher in the wild-type and *ΔcydAB* strains when grown in CO (Figure 1D), suggesting that oxidation of CO by CO dehydrogenase may provide an alternative energy source that enhances biomass generation under these conditions.

In order to determine if additional proteome changes occur during the adaptation of *M. smegmatis* terminal oxidase mutants to CO, we performed proteomic analysis of these strains during exponential growth in the presence and absence of 20% CO. In the absence of CO, the *ΔqcrCAB* mutant significantly increased synthesis of the cytochrome *bd* oxidase subunits CydA (52-fold) and CydB (9.6-fold) compared to the wild-type (Table S1), likely in order to compensate for the loss of the main terminal oxidase. In the Δ*qcrCAB* strain, only 28 proteins significantly differed in abundance in the presence of CO (23 higher, 5 lower) (Figure 2C-E, Table S1), including the same 15 proteins of the *dos* regulon and multiple hypothetical proteins (Figure 2C, D; Table S1). The lack of additional significant changes to the proteome of this strain suggests that it is inherently resistant to CO. In the *ΔcydAB* strain, the abundance of a larger subset of 77 proteins changed in response to CO (47 higher, 30 lower) (Table S1). Most of these differentially regulated proteins are poorly characterised, making it difficult to assess their role in adaptation to CO. Other than the *dos* regulon, the induced proteins include enzymes from the thiamine biosynthetic pathway (ThiC, 8.2-fold; ThiD, 3.7-fold), histidine biosynthetic pathway (HisD, 4.9-fold) and a $NAD(P)^+$ transhydrogenase (6.8-fold) (Table S1), suggesting considerable metabolic remodelling. Overall, the additional proteome changes

observed in the *ΔcydAB* mutant suggest a larger-scale response to cope with increased respiratory inhibition due to the loss of cytochrome *bd* oxidase.

Cytochrome *bd* oxidase is resistant to CO inhibition in actively growing M. *smegmatis* cells

Our finding that in *M. smegmatis* cytochrome *bd* oxidase is important for optimal growth in the presence of CO and is induced under these conditions led us to hypothesise that this enzyme may be inherently resistant to inhibition by CO. To test this hypothesis, O_2 consumption was monitored amperometrically in *M. smegmatis* wild-type, Δ*qcrCAB*, and *ΔcydAB* strains during mid-log phase; cells were spiked with glycerol to simulate respiration, followed by treatment with CO-saturated buffer. Spiking of glycerol stimulated O_2 consumption in all strains (Figure S1). Consistent with a high sensitivity of the cytochrome *bcc-aa*$_3$ complex to inhibition by CO, complete inhibition of O_2 consumption was observed in the *ΔcydAB* mutant upon addition of CO. Inhibition of the wild-type strain was significant but less pronounced than for the *ΔcydAB* mutant, while the Δ*qcrCAB* mutant was not significantly inhibited by CO (Figure 3A). These data are consistent with our hypothesis and indicate that the *M. smegmatis* terminal oxidases are differentiated in their sensitivities to CO poisoning.

Recently, we demonstrated that *M. smegmatis* is able to utilise the trace quantities of CO present in the atmosphere as an energy source during starvation, via the CO dehydrogenase (9). This study demonstrated that the addition of CO leads to enhanced O_2 consumption in *M. smegmatis,* suggesting that electrons derived from CO oxidation enter the respiratory chain, though the specific terminal oxidases

involved in this process were not determined (9). To test this, we spiked carbon-limited (3 days post-OD_{max}) *M. smegmatis* wild-type, Δ*qcrCAB*, and *ΔcydAB* cultures with CO-saturated buffer and amperometrically monitored O_2 consumption. Upon addition of CO, all cultures consumed O_2, with consumption of the *ΔcydAB* culture 1.7-fold less than wild-type (Figure 3B). Conversely, O_2 consumption in the *ΔqcrCAB* culture was 1.5-fold higher than wild-type (Figure 3B). Inhibition of cytochrome *bcc-aa*$_3$ through the addition of zinc azide in the *ΔcydAB* mutant completely abolished CO-dependent O_2 consumption (Figure 3B).

These data demonstrate that electrons generated by CO oxidation by CO dehydrogenase can be donated to either terminal oxidase. Furthermore, the complete inhibition of O_2 consumption by zinc azide in the *ΔcydAB* mutant shows that O_2-dependent CO oxidation is obligately coupled to the terminal oxidases of the respiratory chain. The higher rate of O_2 consumption in the *ΔqcrCAB* mutant may result from the insensitivity of cytochrome *bd* to inhibition by CO. In the wild-type and *ΔcydAB* strains, it is likely that the addition of CO concurrently stimulates O_2 consumption by providing electrons to the electron transport chain and inhibits respiration through inhibition of cytochrome *bcc-aa*$_3$ oxidase. As cytochrome *bd* oxidase is insensitive to CO, in the *ΔqcrCAB* mutant only a stimulatory effect is observed. The respiration observed upon addition of CO to *ΔcydAB* strain during carbon-limitation contrasts with the complete inhibition observed when CO is added to actively growing, glycerol-stimulated cells (Figure 3A, B). This suggests that, as reported for mitochondria (22), differences in the respiratory chain redox state or a higher intracellular O_2 concentration of carbon-starved cells make cytochrome *bcc-aa*$_3$ oxidase less susceptible to inhibition by CO under these conditions.

Discussion

Previous investigations showed that *M. smegmatis,* and mycobacteria more generally, exhibit considerable resistance to CO (8, 9, 16). However, prior to our current work, no underlying mechanism for CO resistance in mycobacteria had been determined. Here we show that induction of cytochrome *bd* oxidase is the key adaptive response for CO resistance in *M. smegmatis*, as the function of this oxidase is largely unaffected by high concentrations of CO. This finding adds to a the growing body of evidence that cytochrome *bd* oxidases play a general role the resistance of the bacterial respiratory chain to gaseous inhibitors (43). The resistance of cytochrome *bd* oxidase to CO in *M. smegmatis* is consistent with a previous report showing that, in *E. coli*, a mutant possessing only cytochrome *bd-I* oxidase is less sensitive to growth inhibition by the CO producing molecule CORM-3 than mutants possessing only the other terminal oxidases (cytochrome *bd-II* and cytochrome *bo'*) of *E. coli* (44). However, a recent study demonstrated that purified cytochrome *bd-I* and *bd-II* oxidases from *E. coli* are more sensitive to inhibition by gaseous CO than cytochrome *bo'* oxidase (45). The difference between these findings may result from the use of CORM-3 for CO delivery in the former study. CORM-3 is known to exert cytotoxic effects independent of CO, making the role of cytochrome *bd-I* oxidase in CO resistance in *E. coli* uncertain (12). As such, our current work represents the first definitive evidence that bacterial cytochrome *bd* oxidases display inherent resistance to CO.

The proteomic analyses showed surprisingly few proteins are differentially abundant in *M. smegmatis* during growth in a 20% CO atmosphere. Fifteen of the most

316 induced proteins, and the only proteins consistently induced in both the wild-type and
317 terminal oxidase mutant backgrounds belong to the *dos* regulon of *M. smegmatis*
318 (17). Considering that our growth data shows that DosR is not required for
319 adaptation to growth in CO, the induction of these proteins is unlikely to be an
320 adaptive response to CO. This further reduces the number of adaptive proteomic
321 changes observed in response to CO. Excluding DosR regulated proteins and
322 cytochrome *bd* oxidase, only 21 proteins are differentially abundant during growth of
323 wild-type *M. smegmatis* in CO, with the majority of these changes less than 5-fold
324 compared to growth in air. This is in contrast to the observation that in *E. coli*
325 approximately 20% of the genome is differentially regulated at a transcriptional level
326 in response to growth in CO (39). This together suggests that, aside from the
327 resistance of its electron transport chain to CO inhibition mediated by cytochrome *bd*
328 oxidase, *M. smegmatis* is otherwise highly resistant to CO.

329 Previously we showed that, in *M. smegmatis*, CO dehydrogenase is active during
330 non-replicative persistence (9). This provides *M. smegmatis* with the ability to utilise
331 CO at atmospheric concentrations (100 ppbv) as an alternative energy source in the
332 absence of organic substrates (9). Our current work shows that electrons derived
333 from CO are donated to O_2 via either of the two terminal oxidases, obligately
334 coupling CO dehydrogenase to the aerobic respiratory chain. The fact that
335 cytochrome *bcc-aa*$_3$ oxidase is able to accept electrons from CO oxidation, despite
336 the fact that it is inhibited by the gas, is seemingly paradoxical. However, CO is a
337 competitive inhibitor of O_2 binding by heme-copper oxidases and CO dehydrogenase
338 in *M. smegmatis* is a high-affinity enzyme that operates at very low CO partial
339 pressures (9, 22). This means that, at the low concentrations of CO that are

340 physiologically relevant for CO dehydrogenase activity in *M. smegmatis*, no
341 significant inhibition of cytochrome *bcc-aa*$_3$ oxidase would be observed.

342 Despite the suggestion that CO has antibacterial potential against pathogenic
343 mycobacteria and numerous other bacterial species (5, 13, 46), surprisingly little is
344 known about physiological and biochemical effects of gaseous CO on the bacterial
345 cell. The uncertainty regarding the effects of CO on bacteria is confounded by the
346 fact that much of the work testing the effects of CO has been performed using
347 CORMs, which have antibiotic activity in addition to the effects of CO release (12). In
348 this work we have shown that *M. smegmatis* has a high level of resistance to CO that
349 requires relatively few changes to its proteome. If these findings extend to
350 pathogenic mycobacteria, then it is unlikely that CO, either produced by the host via
351 heme oxygenase 1 (8) or delivered exogenously, will exert a significant antibacterial
352 effect on pathogenic members of the genus.

Methods

Growth experiments

Mycobacterium smegmatis mc^{2}155 (47), Δ*qcrCAB*, and *ΔcydAB* mutant strains were maintained on lysogeny broth (LB) agar plates supplemented with 0.05% (w/v) Tween80. For broth culture, *M. smegmatis* was grown on Hartmans de Bont minimal medium (48) supplemented with 0.05% (w/v) tyloxapol and 2.9 mM glycerol. Liquid cultures were incubated at 37°C on a rotary incubator at ~180 rpm. For growth assays, triplicate cultures of *M. smegmatis* was grown in 30 mL media in 120 mL sealed serum vials. After inoculation, culture headspace was amended to either 20% CO (*via* 100% v/v CO gas cylinder, 99.999% pure) or 20% N_2 (*via* 100% v/v N_2 cylinder, 99.999% pure). N_2 was added to account for removed O_2. Growth was monitored by measuring optical density (OD) at 600 nm (1 cm cuvettes, Eppendorf BioSpectrometer Basic). When OD_{600} was above 0.5, culture was diluted ten-fold before reading.

Proteomic analysis

For shotgun proteomic analysis, 30 mL cultures of *M. smegmatis* were grown on Hartmans de Bont minimal medium (48) supplemented with 0.05% (w/v) tyloxapol and 5.8 mM glycerol in triplicate in 120 mL serum vials sealed with rubber butyl stoppers. Immediately after inoculation, one triplicate set was amended with 20% CO (*via* 100% v/v CO gas cylinder, 99.999% pure). Cells were harvested in mid-exponential phase (OD_{600} ~0.3) by centrifugation (10,000 × *g*, 10 min, 4 °C). They were subsequently washed in phosphate-buffered saline (PBS; 137 mM NaCl, 2.7 mM KCl, 10 mM Na_2HPO_4 and 2 mM KH_2PO_4, pH 7.4), recentrifuged, and resuspended in 100 mM Tris + 4% SDS at a weight:volume ratio of 1:4. The resultant

suspension was then lysed by beat-beating with 0.1 mm zircon beads for five 30 second cycles. To denature proteins, lysates were boiled at 95 °C for 10 min, then sonicated in a Bioruptor (Diagenode) using 20 cycles of '30 seconds on' followed by '30 seconds off'. The lysates were clarified by centrifugation (14,000 × *g*, 10 mins). Protein concentration was confirmed using the bicinchoninic acid assay kit (Thermo Fisher Scientific) and normalized for downstream analyses. After removal of SDS by chloroform/methanol precipitation, the proteins were proteolytically digested with trypsin (Promega) and purified using OMIX C18 Mini-Bed tips (Agilent Technologies) prior to LC-MS/MS analysis. Using a Dionex UltiMate 3000 RSL Cnano system equipped with a Dionex UltiMate 3000 RS autosampler, the samples were loaded via an Acclaim PepMap 100 trap column (100 µm × 2 cm, nanoViper, C18, 5 µm, 100 Å; Thermo Scientific) onto an Acclaim PepMap RSLC analytical column (75 µm × 50 cm, nanoViper, C18, 2 µm, 100 Å; Thermo Scientific). The peptides were separated by increasing concentrations of buffer B (80% acetonitrile / 0.1% formic acid) for 158 min and analyzed with an Orbitrap Fusion Tribrid mass spectrometer (Thermo Scientific) operated in data-dependent acquisition mode using in-house, LFQ-optimized parameters. Acquired .raw files were analyzed with MaxQuant 1.6.5.0 (ref: PMID: 19029910) to globally identify and quantify proteins pairwise across the different conditions. Data visualization and statistical analyses were performed in R studio (49) with the ggplot2 package (50).

Respirometry measurements

For respirometry measurements, 30 mL cultures of wild-type, Δ*qcrCAB*, and Δ*cydAB* *M. smegmatis* were grown on Hartmans de Bont minimal medium (48) supplemented

401 with 0.05% (w/v) tyloxapol and 5.8 mM glycerol to mid-exponential (OD_{600} = 0.3) or
402 mid-stationary phase (72 hours post OD_{max} ~0.9) in 125 mL aerated conical flasks.
403 Rates of O_2 consumption were measured using a Unisense O_2 microsensor in 1.1
404 mL microrespiration assay chambers that were stirred at 250 rpm at room
405 temperature. Prior to measurement, the electrode was polarized at -800 mV for 1
406 hour with a Unisense multimeter and calibrated with O_2 standards of known
407 concentration. Gas-saturated phosphate-buffered saline (PBS; 137 mM NaCl, 2.7
408 mM KCl, 10 mM Na_2HPO_4, 2 mM KH_2PO_4, pH 7.4) was prepared by bubbling PBS
409 with 100% (v/v) of either O_2 or CO for 5 min. To determine how CO affected
410 respiration in growing cells, 0.9 mL mid-exponential phase cultures of either *M.*
411 *smegmatis* wild-type, Δ*qcrCAB*, or Δ*cydAB* strains and 0.1 mL O_2-saturated PBS
412 were loaded onto respiration chambers and baseline rate of O_2 consumption was
413 measured. Following this, glycerol (3.5 mM final concentration) and 0.1 mL CO-
414 saturated PBS were sequentially amended into the chamber and O_2 consumption
415 was measured before and after addition of CO. To determine the effect of CO in
416 carbon-starved cells, initial oxygen consumption was measured in assay chambers
417 sequentially amended with mid-stationary phase *M. smegmatis* cell suspensions (0.9
418 mL) and O_2-saturated PBS (0.1 mL). After initial measurements, 0.1 mL of CO-
419 saturated PBS was added into the assay mixture. Additionally, O_2 consumption was
420 measured in Δ*cydAB* strain treated with 250 µM zinc azide. Changes in O_2
421 concentrations were recorded using Unisense Logger Software (Unisense,
422 Denmark). Upon observing a linear change in O_2 concentration, rates of
423 consumption were calculated over a period of 20 s and normalized against total
424 protein concentration.

425

Acknowledgements

This work was supported by an ARC DECRA Fellowship (DE170100310; awarded to C.G.), an ARC Discovery Grant (DP200103074; awarded to C.G. and R.G.), an NHMRC EL2 Fellowship (APP1178715; awarded to C.G.), an Australian Government Research Training Program Stipend Scholarship (awarded to K.B.), and a Monash University Doctoral Scholarship (awarded to P.R.F.C.). We thank Prof. Gregory Cook and Dr. Matthew McNeil for providing the Δ*qcrCAB*, Δ*cydAB*, and Δ*dosR* mutants.

Author contributions

C.G. and R.G. conceived and supervised the study. C.G., K.B., P.R.F.C., and R.G. designed experiments. K.B., P.R.F.C., and C.H. performed experiments. K.B., P.R.F.C., C.G., R.G., and C. H. analysed data. K.B., R.G., P.R.F.C., and C.G. wrote the paper with input from all authors.

Data Availability

All raw proteomic data have been deposited at PRIDE with the dataset identifier: PXD018382.

References

1. Prockop LD, Chichkova RI. 2007. Carbon monoxide intoxication: an updated review. J Neurol Sci 262:122-130.
2. Piantadosi CA. 2002. Biological chemistry of carbon monoxide. Antioxidants and Redox Signaling 4:259-270.
3. Dyson PJ, McIndoe JS. 2000. Transition metal carbonyl cluster chemistry, vol 2. CRC Press.
4. Munro AW, Girvan HM, McLean KJ, Cheesman MR, Leys D. 2009. Heme and hemoproteins, p 160-183, Tetrapyrroles. Springer.
5. Chin BY, Otterbein LE. 2009. Carbon monoxide is a poison… to microbes! CO as a bactericidal molecule. Curr Opin Pharmacol 9:490-500.
6. Alonso JR, Cardellach F, López S, Casademont J, Miró Ò. 2003. Carbon monoxide specifically inhibits cytochrome c oxidase of human mitochondrial respiratory chain. Pharmacol Toxicol 93:142-146.
7. Gee DL, Brown WD. 1981. The effect of carbon monoxide on bacterial growth. Meat Sci 5:215-222.
8. Shiloh MU, Manzanillo P, Cox JS. 2008. Mycobacterium tuberculosis senses host-derived carbon monoxide during macrophage infection. Cell host & microbe 3:323-330.
9. Cordero PRF, Bayly K, Leung PM, Huang C, Islam ZF, Schittenhelm RB, King GM, Greening C. 2019. Atmospheric carbon monoxide oxidation is a widespread mechanism supporting microbial survival. The ISME Journal doi:10.1038/s41396-019-0479-8.
10. Desmard M, Davidge KS, Bouvet O, Morin D, Roux D, Foresti R, Ricard JD, Denamur E, Poole RK, Montravers P. 2009. A carbon monoxide-releasing molecule (CORM-3) exerts bactericidal activity against Pseudomonas aeruginosa and improves survival in an animal model of bacteraemia. The FASEB Journal 23:1023-1031.
11. Nobre LS, Seixas JD, Romão CC, Saraiva LM. 2007. Antimicrobial action of carbon monoxide-releasing compounds. Antimicrob Agents Chemother 51:4303-4307.
12. Southam HM, Smith TW, Lyon RL, Liao C, Trevitt CR, Middlemiss LA, Cox FL, Chapman JA, El-Khamisy SF, Hippler M. 2018. A thiol-reactive Ru (II) ion, not CO release, underlies the potent antimicrobial and cytotoxic properties of CO-releasing molecule-3. Redox biology 18:114-123.
13. Desmard M, Foresti R, Morin D, Dagouassat M, Berdeaux A, Denamur E, Crook SH, Mann BE, Scapens D, Montravers P. 2012. Differential antibacterial activity against Pseudomonas aeruginosa by carbon monoxide-releasing molecules. Antioxidants & redox signaling 16:153-163.
14. Percival SL, Williams DW. 2014. Chapter Nine - Mycobacterium, p 177-207. *In* Percival SL, Yates MV, Williams DW, Chalmers RM, Gray NF (ed), Microbiology of Waterborne Diseases (Second Edition) doi:https://doi.org/10.1016/B978-0-12-415846-7.00009-3. Academic Press, London.
15. Annabel B, Anna D, Hannah M. 2019. Global tuberculosis report 2019.
16. Park SW, Hwang EH, Park H, Kim JA, Heo J, Lee KH, Song T, Kim E, Ro YT, Kim SW. 2003. Growth of mycobacteria on carbon monoxide and methanol. J Bacteriol 185:142-147.

17. Berney M, Greening C, Conrad R, Jacobs WR, Cook GM. 2014. An obligately aerobic soil bacterium activates fermentative hydrogen production to survive reductive stress during hypoxia. Proceedings of the National Academy of Sciences 111:11479-11484.
18. Cook GM, Hards K, Vilchèze C, Hartman T, Berney M. 2014. Energetics of Respiration and Oxidative Phosphorylation in Mycobacteria. Microbiology spectrum 2:10.1128/microbiolspec.MGM2-0015-2013.
19. Matsoso LG, Kana BD, Crellin PK, Lea-Smith DJ, Pelosi A, Powell D, Dawes SS, Rubin H, Coppel RL, Mizrahi V. 2005. Function of the Cytochrome bc_1-aa_3 Branch of the Respiratory Network in Mycobacteria and Network Adaptation Occurring in Response to Its Disruption. Journal of Bacteriology 187:6300-6308.
20. Giuffrè A, Borisov VB, Arese M, Sarti P, Forte E. 2014. Cytochrome bd oxidase and bacterial tolerance to oxidative and nitrosative stress. Biochimica et Biophysica Acta (BBA)-Bioenergetics 1837:1178-1187.
21. Safarian S, Hahn A, Mills D, Radloff M, Eisinger ML, Nikolaev A, Meier-Credo J, Melin F, Miyoshi H, Gennis R. 2019. Active site rearrangement and structural divergence in prokaryotic respiratory oxidases. Science 366:100-104.
22. Cooper CE, Brown GC. 2008. The inhibition of mitochondrial cytochrome oxidase by the gases carbon monoxide, nitric oxide, hydrogen cyanide and hydrogen sulfide: chemical mechanism and physiological significance. J Bioenerg Biomembr 40:533.
23. Quesada A, Guijo MI, Merchán F, Blázquez B, Igeño MI, Blasco R. 2007. Essential role of cytochrome bd-related oxidase in cyanide resistance of Pseudomonas pseudoalcaligenes CECT5344. Appl Environ Microbiol 73:5118-5124.
24. Mason MG, Shepherd M, Nicholls P, Dobbin PS, Dodsworth KS, Poole RK, Cooper CE. 2009. Cytochrome bd confers nitric oxide resistance to Escherichia coli. Nat Chem Biol 5:94.
25. Korshunov S, Imlay KR, Imlay JA. 2016. The cytochrome bd oxidase of Escherichia coli prevents respiratory inhibition by endogenous and exogenous hydrogen sulfide. Mol Microbiol 101:62-77.
26. Kumar A, Deshane JS, Crossman DK, Bolisetty S, Yan B-S, Kramnik I, Agarwal A, Steyn AJ. 2008. Heme oxygenase-1-derived carbon monoxide induces the Mycobacterium tuberculosis dormancy regulon. Journal of biological chemistry 283:18032-18039.
27. Madrona Y, Waddling CA, de Montellano PRO. 2016. Crystal structures of the CO and NOBound DosS GAF-A domain and implications for DosS signaling in Mycobacterium tuberculosis. Arch Biochem Biophys 612:1-8.
28. Kumar A, Toledo JC, Patel RP, Lancaster JR, Steyn AJ. 2007. Mycobacterium tuberculosis DosS is a redox sensor and DosT is a hypoxia sensor. Proceedings of the National Academy of Sciences 104:11568-11573.
29. Boon C, Dick T. 2002. Mycobacterium bovis BCG response regulator essential for hypoxic dormancy. J Bacteriol 184:6760-6767.
30. Rustad TR, Harrell MI, Liao R, Sherman DR. 2008. The enduring hypoxic response of Mycobacterium tuberculosis. PLoS ONE 3.
31. Cordero PR, Grinter R, Hards K, Cryle MJ, Warr CG, Cook GM, Greening C. 2019. Two uptake hydrogenases differentially interact with the aerobic

542 respiratory chain during mycobacterial growth and persistence. J Biol Chem
543 294:18980-18991.
544 32. Greening C, Berney M, Hards K, Cook GM, Conrad R. 2014. A soil
545 actinobacterium scavenges atmospheric H2 using two membrane-associated,
546 oxygen-dependent [NiFe] hydrogenases. Proceedings of the National
547 Academy of Sciences 111:4257-4261.
548 33. Berney M, Greening C, Hards K, Collins D, Cook GM. 2014. Three different
549 [NiFe] hydrogenases confer metabolic flexibility in the obligate aerobe M
550 ycobacterium smegmatis. Environmental microbiology 16:318-330.
551 34. Harold LK, Antoney J, Ahmed FH, Hards K, Carr PD, Rapson T, Greening C,
552 Jackson CJ, Cook GM. 2019. FAD-sequestering proteins protect
553 mycobacteria against hypoxic and oxidative stress. J Biol Chem 294:2903-
554 2912.
555 35. Chauviac F-X, Bommer M, Yan J, Parkin G, Daviter T, Lowden P, Raven EL,
556 Thalassinos K, Keep NH. 2012. Crystal structure of reduced MsAcg, a
557 putative nitroreductase from Mycobacterium smegmatis and a close
558 homologue of Mycobacterium tuberculosis Acg. J Biol Chem 287:44372-
559 44383.
560 36. Greening C, Villas-Bôas SG, Robson JR, Berney M, Cook GM. 2014. The
561 growth and survival of Mycobacterium smegmatis is enhanced by co-
562 metabolism of atmospheric H2. PLoS ONE 9:e103034.
563 37. Poweleit N, Czudnochowski N, Nakagawa R, Trinidad DD, Murphy KC,
564 Sassetti CM, Rosenberg OS. 2019. The structure of the endogenous ESX-3
565 secretion system. Elife 8.
566 38. Chai A-F, Bulloch EM, Evans GL, Lott JS, Baker EN, Johnston JM. 2015. A
567 covalent adduct of MbtN, an acyl-ACP dehydrogenase from Mycobacterium
568 tuberculosis, reveals an unusual acyl-binding pocket. Acta Crystallographica
569 Section D: Biological Crystallography 71:862-872.
570 39. Wareham LK, Begg R, Jesse HE, Van Beilen JW, Ali S, Svistunenko D,
571 McLean S, Hellingwerf KJ, Sanguinetti G, Poole RK. 2016. Carbon monoxide
572 gas is not inert, but global, in its consequences for bacterial gene expression,
573 iron acquisition, and antibiotic resistance. Antioxidants & redox signaling
574 24:1013-1028.
575 40. Mohan A, Padiadpu J, Baloni P, Chandra N. 2015. Complete genome
576 sequences of a Mycobacterium smegmatis laboratory strain (MC2 155) and
577 isoniazid-resistant (4XR1/R2) mutant strains. Genome Announc 3:e01520-14.
578 41. Zacharia VM, Manzanillo PS, Nair VR, Marciano DK, Kinch LN, Grishin NV,
579 Cox JS, Shiloh MU. 2013. cor, a novel carbon monoxide resistance gene, is
580 essential for Mycobacterium tuberculosis pathogenesis. MBio 4:e00721-13.
581 42. Lu P, Heineke MH, Koul A, Andries K, Cook GM, Lill H, Van Spanning R, Bald
582 D. 2015. The cytochrome bd-type quinol oxidase is important for survival of
583 Mycobacterium smegmatis under peroxide and antibiotic-induced stress.
584 Scientific reports 5:10333.
585 43. Forte E, Borisov VB, Vicente JB, Giuffrè A. 2017. Cytochrome bd and
586 gaseous ligands in bacterial physiology, p 171-234, Adv Microb Physiol, vol
587 71. Elsevier.
588 44. Jesse HE, Nye TL, McLean S, Green J, Mann BE, Poole RK. 2013.
589 Cytochrome bd-I in Escherichia coli is less sensitive than cytochromes bd-II or
590 bo′ 'to inhibition by the carbon monoxide-releasing molecule, CORM-3: N-
591 acetylcysteine reduces CO-RM uptake and inhibition of respiration.

592 Biochimica et Biophysica Acta (BBA)-Proteins and Proteomics 1834:1693-
593 1703.
594 45. Forte E, Borisov VB, Siletsky SA, Petrosino M, Giuffrè A. 2019. In the
595 respiratory chain of Escherichia coli cytochromes bd-I and bd-II are more
596 sensitive to carbon monoxide inhibition than cytochrome bo3. Biochimica et
597 Biophysica Acta (BBA)-Bioenergetics 1860:148088.
598 46. Zacharia VM, Shiloh MU. 2012. Effect of carbon monoxide on Mycobacterium
599 tuberculosispathogenesis. Medical gas research 2:30.
600 47. Snapper SB, Melton RE, Mustafa S, Kieser T, Jr WRJ. 1990. Isolation and
601 characterization of efficient plasmid transformation mutants of *Mycobacterium*
602 *smegmatis*. Molecular Microbiology 4:1911-1919.
603 48. Hartmans S, De Bont JA. 1992. Aerobic vinyl chloride metabolism in
604 Mycobacterium aurum L1. Applied and environmental microbiology 58:1220-
605 1226.
606 49. R Core Team. 2018. R: A Language and Environment for Statistical
607 Computing, R Foundation for Statistical Computing, Vienna, Austria.
608 https://www.R-project.org/.
609 50. Wickham H. 2016. ggplot2: Elegant Graphics for Data Analysis. Springer-
610 Verlag New York.

611

Figures

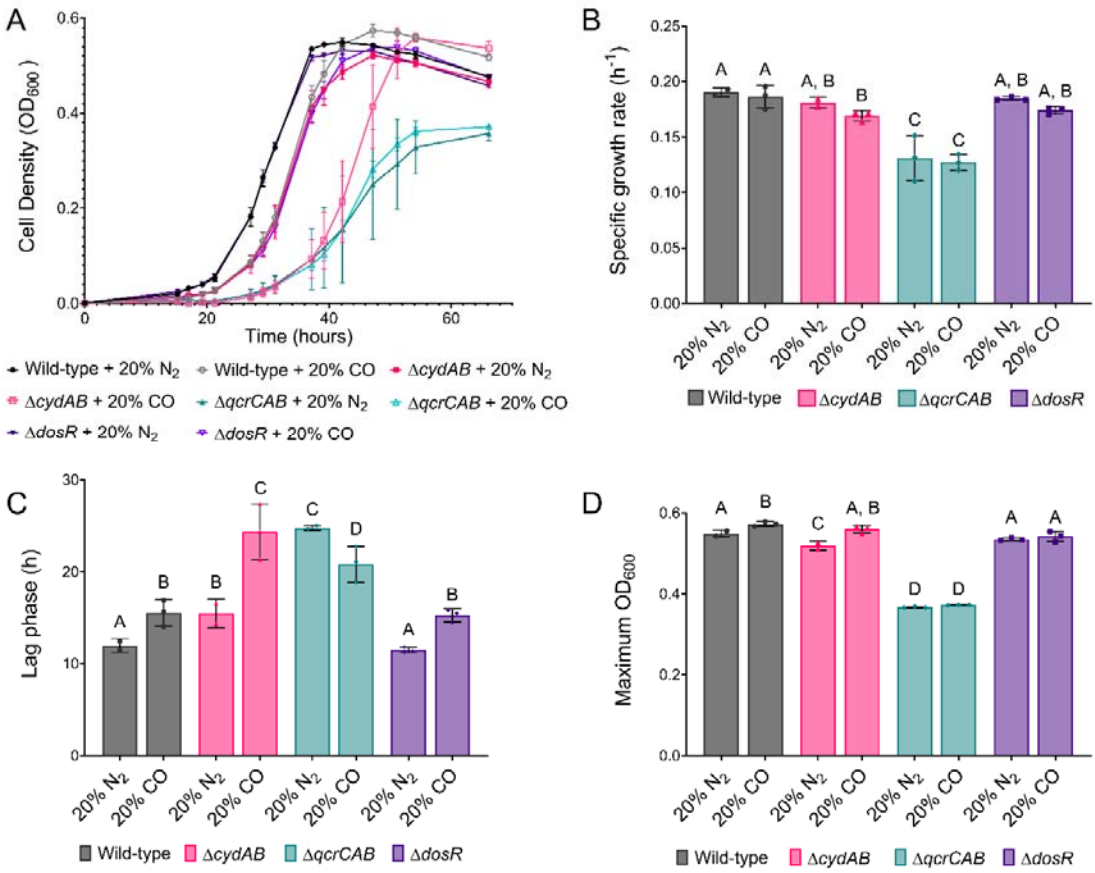

Figure 1. Growth of *M. smegmatis* wild-type and terminal oxidase mutants in air supplemented with either 20% CO or 20% N_2. (A) Growth curves of *M. smegmatis* wild-type, terminal oxidase, and *dosR* mutants grown in sealed culture vials in the presence of air supplemented with 20% CO or 20% N_2. The specific growth rate (B), length of lag phase (C) and maximum culture density (D) for each strain is also shown. *Different letters above data bars (A , B, C, D) designate significantly different values (p-value <0.05, two-way ANOVA).*

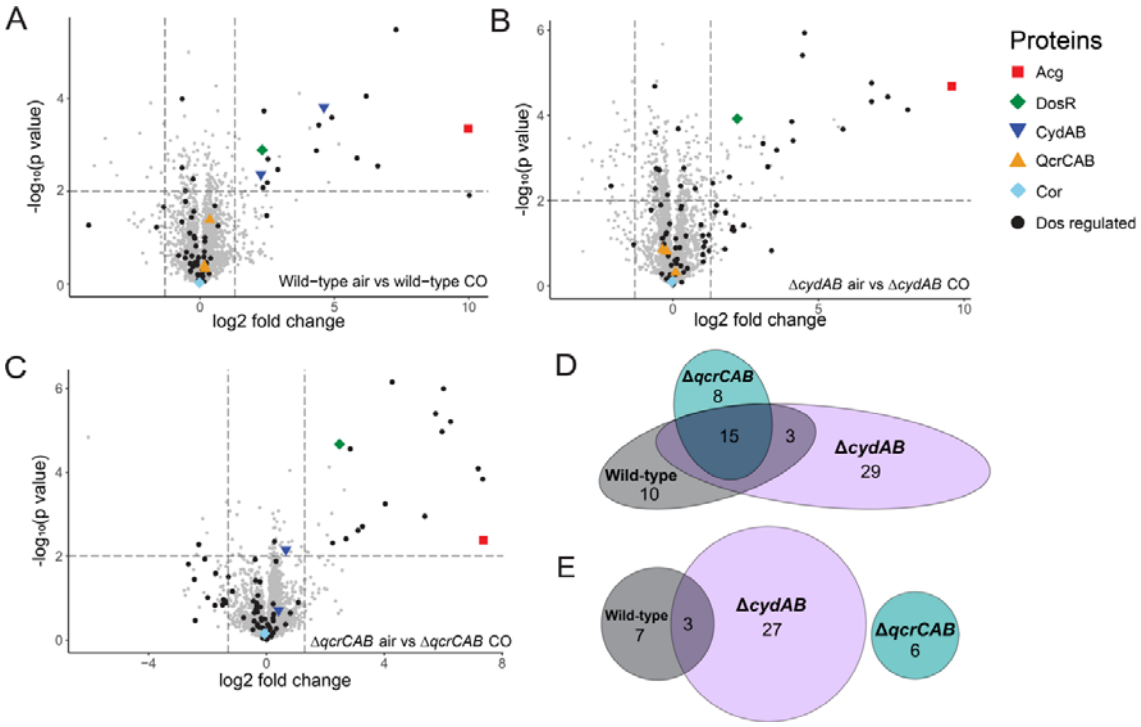

622

623 **Figure 2. Shotgun proteomic analysis of *M. smegmatis* wild-type and terminal**
624 **oxidase mutants at mid-log phase grown in air in the presence and absence of**
625 **20% CO.** Volcano plots showing differential detection of proteins in (A) wild-type, (B)
626 *ΔcydAB*, and (C) *ΔqcrCAB* strains in air in with and without 20% CO. Each protein is
627 represented by a single point. DosS/DosR regulon proteins are represented by black
628 dots, and proteins of interest are highlighted as per the legend. Strains were
629 harvested at mid-exponential phase (OD_{600} ~0.3). Venn diagrams showing overlap of
630 proteins identified by the shotgun proteomics with higher (D) and lower (E)
631 abundances in wild-type, *ΔqcrCAB*, *ΔcydAB* mutant strains grown in air + 20% CO.

632

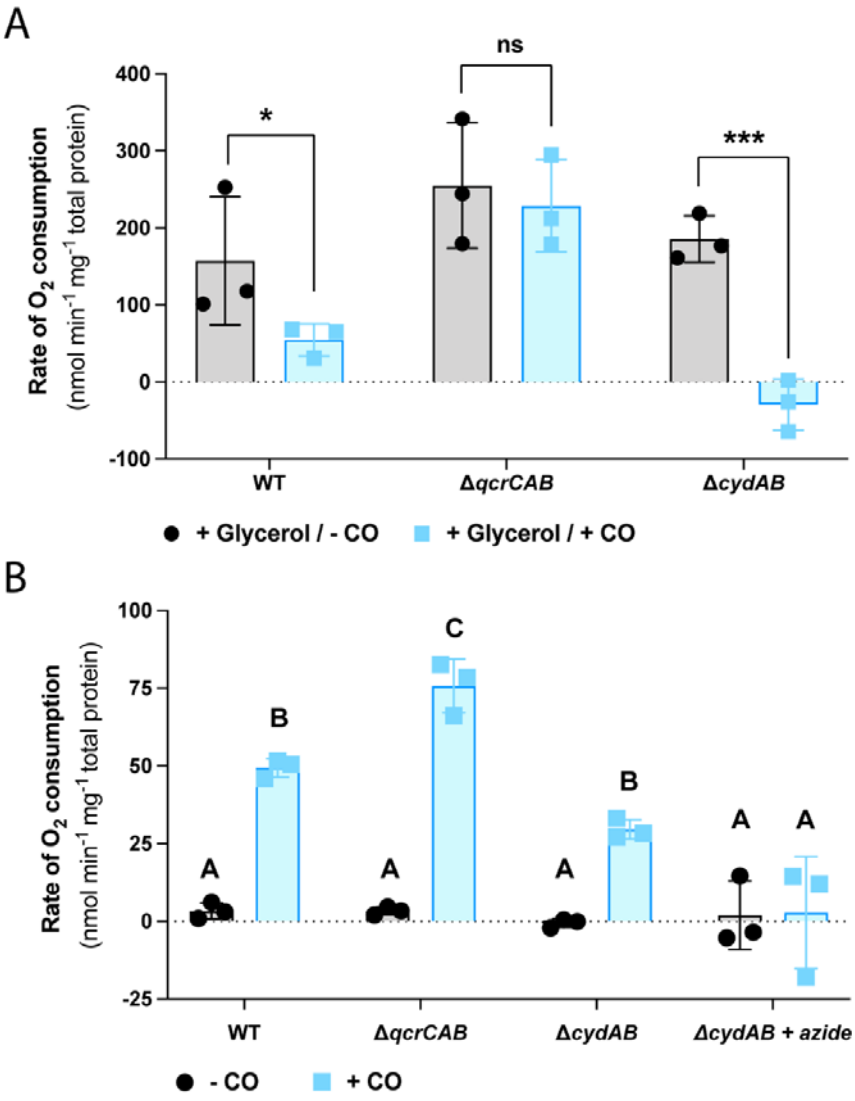

633

634 **Figure 3. Oxygen consumption of *M. smegmatis* terminal oxidases in the**
635 **presence of CO** (A) Rate of O_2 consumption by *M. smegmatis* wild-type, *ΔqcrCAB*,
636 *and ΔcydAB* mid-exponential, glycerol-spiked cultures in the presence and absence
637 of CO. ns = non-significant, * = $p < 0.05$, *** = $p < 0.0005$ (B) Rates of O_2
638 consumption of carbon-starved (3-days post OD_{max}) *M. smegmatis* wild-type,
639 *ΔqcrCAB,* and *ΔcydAB* cultures before and after spiking with CO. O_2 consumption
640 was measured with an oxygen electrode. Azide is a compound that targets the *bcc-*
641 aa_3 cytochrome oxidase and therefore acts as a negative control. Error bars

represent standard deviation of three biological replicates. *Different letters above data bars (A , B, C) designate to significantly different values (p-value <0.05, two-way ANOVA).*

Supplemental Data

Table S1. Summary of shotgun proteomic data (xlsx file).

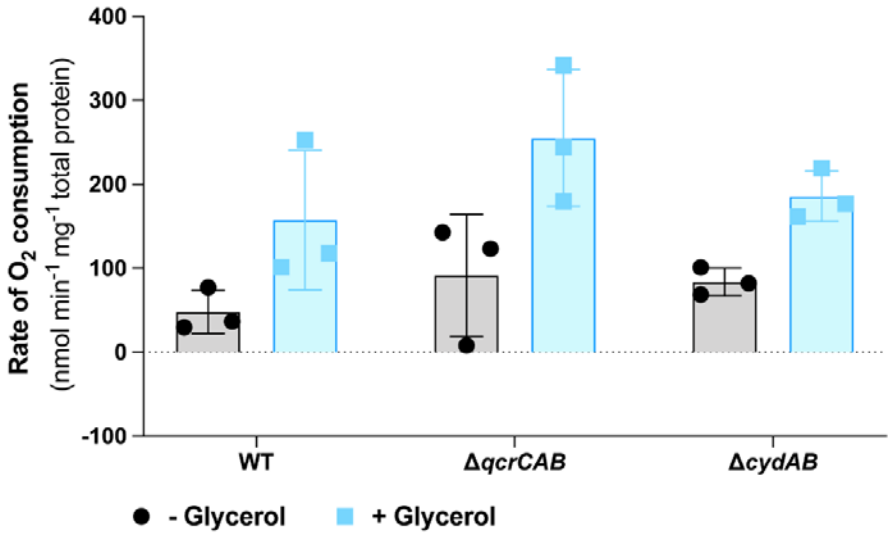

Figure S1. Stimulation of O_2 in *M. smegmatis* upon addition of glycerol. The specific O_2 consumption rate of mid-exponential phase *M. smegmatis* wild-type and terminal oxidase mutants, before and after the addition of 3.5 mM glycerol.